

# Frictionless motion of lattice defects

N.Gorbushin,<sup>1</sup> G. Mishuris,<sup>2</sup> and L. Truskinovsky<sup>1</sup>

<sup>1</sup>*PMMH, CNRS – UMR 7636, CNRS, ESPCI Paris, PSL Research University, 10 rue Vauquelin, 75005 Paris, France*

<sup>2</sup>*Department of Mathematics, Aberystwyth University, Ceredigion SY23 3BZ, Wales, UK*

(Dated: June 24, 2020)

Energy dissipation by fast crystalline defects takes place mainly through the resonant interaction of their cores with periodic lattice. We show that the resultant effective friction can be reduced to zero by appropriately tuned acoustic sources located on the boundary of the body. To illustrate the general idea, we consider three prototypical models describing the main types of strongly discrete defects: dislocations, cracks and domain walls. The obtained control protocols, ensuring dissipation-free mobility of topological defects, can be also used in the design of meta-material systems aimed at transmitting mechanical information.

Mobile crystalline defects respond to lattice periodicity by dynamically adjusting their core structure which leads to radiation of lattice waves through parametric resonance [1–5]. Such ‘hamiltonian damping’ is one of the main mechanisms of energy loss for fast moving dislocations [6, 7], crack tips [8, 9] and elastic phase/twin boundaries [10, 11]. Similar effective dissipation hinders the mobility of topological *defects* in mesoscopic dispersive systems, from periodically modulated composites[12] to discrete acoustic metamaterials [13].

While at the macroscale friction is usually diminished by applying lubricants, at the microscale it may be preferable to use instead external sources of ultrasound (sonolubricity) [14]. Correlated mechanical vibrations are known to reduce *macroscopic* friction through acoustic unjamming [15] as in the case of the remote triggering of earthquakes [16]. General detachment front tips serve as macroscopic defects whose mobility in highly inhomogeneous environments can be controlled by AC (alternating current) driving [17]. Ultrasound-induced lubricity can also reduce friction at the microscale [18]. It is known, for instance, that the forming load drops significantly in the presence of appropriately tuned time-periodic driving which reduces dislocation friction [19].

The AC-based control of the directed transport in *damped* systems was studied extensively for the case when the sources are distributed in the bulk [20–22]. In this Letter we neglect the conventional bulk dissipation, associated for instance, with ‘phonon wind’ [23], and show how in purely Hamiltonian setting the effective friction can be tuned to zero by the special AC driving acting on the system boundary [24, 25].

Since classical continuum models lack the resolution to describe dynamic defect cores and therefore cannot capture adequately the interaction between the defect and the external micro-structure, we use atomistic models accounting for the coupling between the defect and the lattice vibrations while respecting the anharmonicity of interatomic forces. We build upon the theoretical methodology developed in [10, 26, 27] and show that such driving can compensate radiative damping *completely*, making the discrete system fully transparent for mobile topological defects.

To highlight ideas we present a comparative study of the three prototypical snapping-bond type lattice models originating in crystal plasticity (Frenkel-Kontorova (FK) model [7]),

theory of structural phase transitions (bi-stable Fermi-Pasta-Ulam (FPU) model [28]) and fracture mechanics (Peyrard-Bishop (PB) model, [29]).

In the individual setting of each of these models we study the effect of the boundary AC sources on kinetic/mobility laws for the corresponding lattice defects. The latter relate the macroscopic driving force (dynamic generalization of the Peach-Koehler force in the case of dislocations, the stress intensity factor in the case of cracks and the Eshelby force in the case of phase boundaries) and the velocity of the defect. We find that in the presence of AC sources such relations becomes *multivalued*. We focus particularly on designing the AC protocols which ensure that the steady propagation of a defect takes place under *zero* driving force.

The possibility of externally guided radiation-free propagation of mechanical information is presently of considerable interest for designing discrete meta-materials with buckling linkages. Geometric phase transitions generating information-carrying defects in such systems play a central role in a multitude of new applications from recoverable energy harvesting to controlled structural collapse [30–32].

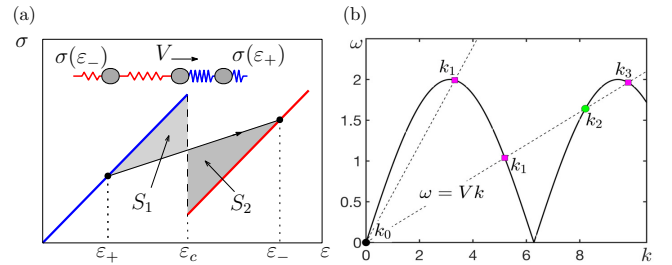


Figure 1: (a) Piece-wise linear stress-strain relation  $\sigma = \sigma(\varepsilon)$ ; the macroscopic driving force  $G^M(V) = S_2 - S_1$ . (b) Dispersion relation  $\omega(k)$  for  $\text{Im}(k) = 0$  (acoustic branch);  $k_j$  correspond to the radiated waves in cases  $K = 1$  and  $K = 3$ , see the text. Green circles correspond to AC sources behind the defect, magenta squares – ahead of the defect.

The FPU model with bi-stable interactions is used to represent the simplest crystal defect, a domain wall [11, 33]. In terms of dimensionless particle displacements  $u_j(t)$  the dynamics is described by the system

$$\ddot{u}_j(t) = \sigma(u_{j+1} - u_j) - \sigma(u_j - u_{j-1}). \quad (1)$$

It will be convenient to use strain variables  $\varepsilon_j(t) = u_{j+1}(t) - u_j(t)$  and introduce the strain energy density  $w(\varepsilon)$  so that  $\sigma(\varepsilon_j) = w'(\varepsilon_j)$ . For analytical transparency we adopt the simplest bi-quadratic model with  $w = (1/2)\varepsilon^2 - \sigma_0(\varepsilon - \varepsilon_c)H(\varepsilon - \varepsilon_c)$ , where  $H(x)$  is the Heaviside function,  $\varepsilon_c$  is the characteristic strain and  $\sigma_0$  is the stress drop, see Fig. 1(a).

We search for traveling wave (TW) solutions of (1) in the form  $u_j(t) = u(\eta)$  and  $\varepsilon_j = \varepsilon(\eta)$ , where  $\eta = j - Vt$  and  $V < 1$  is the normalized velocity of the defect. If we associate the defect with  $\eta = 0$  the equation for the strain field reduces to  $V^2 d^2 \varepsilon / d\eta^2 = \sigma(\eta+1) + \sigma(\eta-1) - 2\sigma(\eta)$ , where  $\sigma(\eta) = \varepsilon(\eta) - \sigma_0 H(-\eta)$ . When this linear equation is solved, the velocity  $V$  is found from the nonlinear *switching* condition  $\varepsilon(0) = \varepsilon_c$ .

Using the Fourier transform  $\hat{f}(k) = \int_{-\infty}^{\infty} f(\eta) e^{ik\eta} d\eta$ , we can rewrite the main linear problem in the form  $L(k)\hat{\varepsilon}(k) = \sigma_0 \omega^2(k)/(0+ik)$ , where  $L(k) \equiv \omega^2(k) - (kV)^2$  and  $\omega^2(k) = 4 \sin^2(k/2)$  is the dispersion relation represented in this case by a single acoustic branch, see Fig. 1(b). The strain field  $\varepsilon(\eta)$  can be decomposed into a sum of the term  $\varepsilon_{in}(\eta)$ , which is due to inhomogeneity (mimicking nonlinearity) and the term  $\varepsilon_{dr}(\eta)$ , due to the combined action of DC (direct current) and AC driving. The former can be written explicitly

$$\varepsilon_{in}(\eta) = \frac{\sigma_0}{2\pi} \int_{-\infty}^{\infty} \frac{\omega^2(k) e^{-ik\eta}}{(0+ik)L(k)} dk. \quad (2)$$

The latter must satisfy  $L(k)\hat{\varepsilon}_{dr}(k) = 0$  which in the physical space gives

$$\varepsilon_{dr}(\eta) = \sum_{j=1}^K A_j \sin(k_j \eta + \varphi_j) + C. \quad (3)$$

The constants  $A_j$  and  $\varphi_j$  describe the amplitude and the phase of the incoming waves generated at the distant boundaries. They represent the AC driving which is characterized by the wave numbers  $k_j$  that are taken among the positive real roots of the kernel  $L(k)$ : if  $\omega'(k_j)$  is smaller (greater) than  $V$  the sources are in front of (behind) the moving defect. The constant  $C$  in (3), representing the root  $k_0 = 0$ , controls the uniform strain ahead of the moving defect and represents the DC driving.

Use the switching condition we can obtain the explicit relations for the limiting strains in the form  $\langle \varepsilon \rangle(\pm\infty) \equiv \varepsilon_{\pm} = \varepsilon_c \mp \frac{1}{2} \frac{\sigma_0}{1-V^2} + \sigma_0 Q - \sum_{j=1}^K A_j \sin \varphi_j$ , where  $\langle f \rangle = \lim_{T \rightarrow \infty} (1/T) \int_0^T f(s) ds$  and the expression for the universal function  $Q(V)$  can be found in [34]. It can be checked that the obtained solution respects the macroscopic momentum balance represented by one of the Rankine-Hugoniot (RH) conditions [35]:  $V^2 = (\sigma(\varepsilon_+) - \sigma(\varepsilon_-))/(\varepsilon_+ - \varepsilon_-)$ . The limiting values of the mass velocity  $v_j = \dot{u}_j$  naturally satisfy another (kinematic) RH condition  $\langle v \rangle(\pm\infty) \equiv v_{\pm} = -V\varepsilon_{\pm}$ .

We now write the macroscopic energy dissipation on the moving defects as  $\mathcal{R} = VG \geq 0$  where  $G$  is the driving force. In the absence of the AC driving ( $A_j = 0$ ) we obtain  $G =$

$G^M$ , where

$$G^M = \llbracket w \rrbracket - \{\sigma\} \llbracket \varepsilon \rrbracket, \quad (4)$$

and we used the standard notations  $\llbracket f \rrbracket = f_+ - f_-$  and  $\{f\} = (f_+ + f_-)/2$  [36]. In our case  $G^M = (\sigma_0/2)(\varepsilon_+ + \varepsilon_- - 2\varepsilon_c)$ . With the AC driving present, we need to write  $\mathcal{R} = V(G^M + G^m) \geq 0$  where the total power exerted by microscopic sources is

$$VG^m = \sum_{j=1}^K (1/2) A_j^2 |\omega'(k_j) - V| \geq 0. \quad (5)$$

The relation for  $\mathcal{R}$  can be checked by the independent computation of the energy carried by the microscopic radiation away from the moving defect to infinity [34].

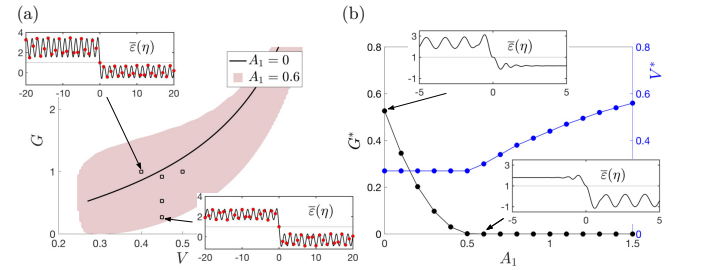


Figure 2: (a) Kinetic domain for the case  $K = 1$ , open squares show the selected TW solutions reached numerically [34]; (b) Amplitude dependence of  $G^*$  and  $V^*$ ; insets show normalized strains  $\bar{\varepsilon}(\eta) = \varepsilon(\eta)/\varepsilon_c$ . Parameters:  $\sigma_0 = 2$ ,  $\varepsilon_c = 1$ .

The dependence of  $G$  on  $V$  for a high velocity subset of admissible solutions is shown in Fig. 2(a). The radiative damping is represented here by a single wave number  $k_1$ . The AC driving is tuned to the same wave number and its source is placed ahead of the moving defect (the  $K = 1$  regime). If the AC driving is absent and all  $A_j = 0$ , there is a single value of  $V$  for each value of  $G$  within the admissible range  $\pm(\varepsilon_c - \varepsilon(\eta)) > 0$  at  $\pm\eta > 0$ . Even if only one coefficient  $A_1 \neq 0$ , each admissible value of velocity  $V$  can be reached within a finite range of DC driving amplitudes with the associated phase shift  $\varphi_1$  varying continuously. In this case the *kinetic relation* transforms into a 2D *kinetic domain*, see Fig. 2(a), where by fixing the DC drive we can either speed up or slow down the defect as we change the frequency of the AC source.

The possibility of the AC induced friction *reduction* is seen from the fact that for each  $V$  there is a range of the admissible driving forces  $G$  with the minimal value  $G^*(V)$ . Moreover, for some  $V^*$  such friction can be eliminated completely if the amplitude  $A_1$  reaches beyond a threshold. Note that the emergence of friction-free regimes resembles a second order phase transition with the dissipation  $G^*$  as the order parameter, see Fig. 2(b). The non-dissipative regimes with  $K = 1$  are naturally anti-phase with respect to the radiated waves so that  $\varphi_1^* = \pi/2$ , see a typical strain distribution in the insets

in Fig. 2(b) and Fig. 3. The relation between the AC amplitude and the defect velocity for such regimes can be written explicitly  $A_1^* = \sigma_0 V / (V - \omega'(k_f))$ .

In the general case  $K \neq 1$  the number of dissipative waves is odd and the dissipation-free regimes also must have an odd number of AC sources to cancel each of these waves. Consider, for instance, the case  $K = 3$ , illustrated in Fig. 1(b), where two dissipative lattice waves ( $k_1$  and  $k_3$ ) release energy at  $-\infty$  and one wave ( $k_2$ ) - at  $+\infty$ . To block these dissipative waves one must have the sources of AC driving both in front and behind the defect. The corresponding amplitudes, ensuring that  $G^*(V) = 0$ , are  $A_j^* = (-1)^j \sigma_0 V / (\omega'(k_j) - V)$  with  $j = 1, 2, 3$ , see Fig. 3.

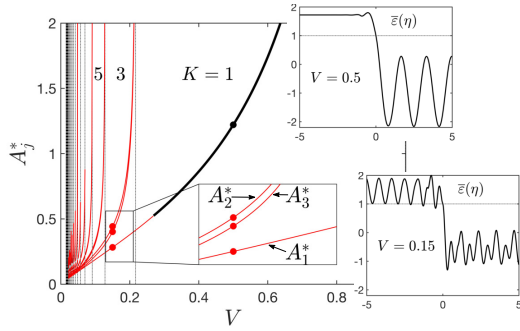


Figure 3: Amplitudes of the AC sources  $A_j^*(V)$ ,  $j = 1, 2, \dots, K$  for  $K = 1, 3, 5, \dots$ ; insets show strains  $\bar{\varepsilon}(\eta) = \varepsilon(\eta)/\varepsilon_c$  at  $V = 0.15$  and  $V = 0.5$  with corresponding  $A_j^*$  marked by solid circles. Black lines correspond to admissible solutions, red - to non admissible. Parameters:  $\sigma_0 = 2$ ,  $\varepsilon_c = 1$ .

The numerical check shows that the admissible frictionless regimes exist only for  $K = 1$ . To show numerical stability of these regimes we simulated the transient problem with initial data close to the analytical TW solutions, see [34] for details. The simulation involving 1000 equations and showing stable dissipation-free propagation of the defect is presented in the form of the supplementary Movie 2.

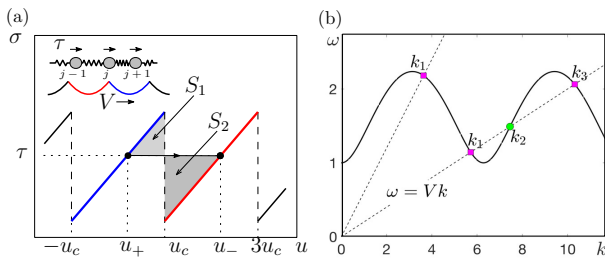


Figure 4: (a) Dislocation propagation driven by the constant force  $\tau$ ; macroscopic driving force  $G^M(V) = S_2 - S_1$ ; (b) Dispersion relation for  $\text{Im}(k) = 0$  (optical branch). The wave numbers  $k_j$  define waves radiated in the cases  $K = 1$  and  $K = 3$ .

The simplest FK model [6, 37] can be used to analyze the frictionless propagation regimes for moving dislocations, see Fig. 4(a). To describe a single dislocation we only need two wells of the on-site periodic potential. The displacement

$u_j(t)$ , describing horizontal slip, must solve the equations

$$\ddot{u}_j = u_{j-1} + u_{j+1} - 2u_j - \sigma(u_j) + \tau \quad (6)$$

where  $\tau$  is a uniform load. The function  $\sigma(u)$  is illustrated in Fig. 4(a) and is defined via the on-site potential  $w(u) = (1/2)u^2$  when  $-u_c < u < u_c$  and  $w(u) = (1/2)u^2 - \sigma_0(u - u_c)$  when  $u_c < u < 3u_c$  representing the two relevant periods. We again use the TW ansatz  $u_j(t) = u(\eta)$ ,  $\eta = j - Vt$  and apply the corresponding condition of admissibility. Unlike the previous case, the DC drive  $\tau$  is now applied in the bulk.

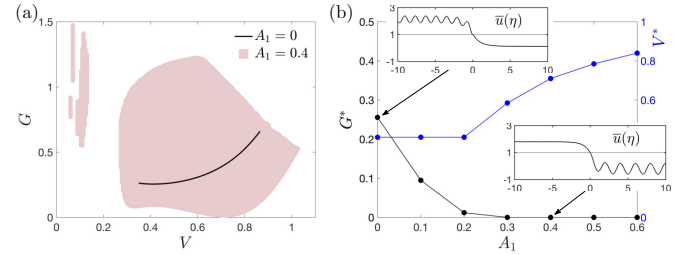


Figure 5: (a) Kinetic domains for dislocations showing admissible solutions with  $K = 1$ . There is only one damping wave in the big pink domain and more than one in the smaller ones. (b) AC amplitude dependence of  $G^*(V^*)$  and  $V^*$ ; insets show displacements  $\bar{u}(\eta) = u(\eta)/u_c$ . Parameters:  $\sigma_0 = 2$ ,  $u_c = 1$ .

We need to solve the linear equation  $V^2 u''(\eta) = u(\eta + 1) + u(\eta - 1) - 3u(\eta) + \sigma_0 H(-\eta) + \tau$  and then find the defect velocity  $V$  using the nonlinear *switching* condition  $u(0) = u_c$ . The solution can be again represented in the form  $u(\eta) = u_{in}(\eta) + u_{dr}(\eta)$ . The first term, which is due to inhomogeneity (mimicking nonlinearity) now includes the DC driving  $\tau$ :

$$u_{in}(\eta) = \tau + \frac{\sigma_0}{2\pi} \int_{-\infty}^{\infty} \frac{e^{-ik\eta}}{(0 + ik)L(k)} dk, \quad (7)$$

where the operator  $L(k)$  remains the same as in the FPU problem but the dispersion relation  $\omega^2(k) = 4\sin^2(k/2) + 1$  is now represented by a single optical branch. The second term responsible for the AC driving must again satisfy  $L(k)\hat{u}_{dr}(k) = 0$  and can be again represented as a combination of linear waves whose phase velocity is equal to  $V$

$$u_{dr}(\eta) = \sum_{j=1}^K A_j \sin(k_j \eta + \varphi_j). \quad (8)$$

Here  $k_j$  are again the positive real roots of  $L(k) = 0$ .

Using the switching condition we obtain for the time averaged displacements at  $\pm\infty$  the values  $u_{\pm} = u_c \mp (\sigma_0/2) + \sigma_0 R - \sum_j A_j \sin \varphi_j$  with the explicit expression for the universal function  $R(V)$  is given again in [34]. The analogs of the RH conditions are now  $u_+ = \tau$  and  $u_- = \tau + \sigma_0$ .

If we denote the stress in the horizontal bonds by  $\bar{\sigma}(\varepsilon) = \varepsilon$  we can write the rate of dissipation at the macro-scale as

$VG^M = \llbracket v^2/2 + \varepsilon^2/2 + w - \tau u \rrbracket V + \llbracket \bar{\sigma} v \rrbracket$ . Applying the kinematic RH condition  $\llbracket v \rrbracket + V \llbracket \varepsilon \rrbracket = 0$  we obtain

$$G^M = \llbracket w \rrbracket - \tau \llbracket u \rrbracket. \quad (9)$$

Since  $\varepsilon_{\pm} = \bar{\sigma}(\varepsilon_{\pm}) = 0$  we can finally write the macroscopic driving force in the form  $G^M = \sigma_0^2/2 - \sigma_0(u_c - u_+)$ . The contribution to the energy flux due to AC sources is now

$$VG^m = \sum_{j=1}^K (1/2) A_j^2 \omega^2(k_j) |\omega'(k_j) - V| \geq 0. \quad (10)$$

The multi-valued relation  $\mathcal{R}(V) = VG(V) = G^M(V) + G^m(V)$  for admissible solutions is illustrated in Fig. 5(a) for the case  $K = 1$ . It is again possible to completely cancel the lattice friction and obtain regimes with  $G^*(V^*) = 0$ . In such regimes, illustrated for  $K = 1$  in Fig. 5(b), the radiated waves are again annihilated by the waves generated by the AC source with the amplitudes  $A_j^* = (-1)^j \sigma_0 V / (\omega(k_j)^2 (\omega'(k_j) - V))$  and phase shifts  $\varphi_j^* = \pi/2$ .

Our last example deals with reversible fracture in the simplest PB-type setting [9, 29, 38]. The lattice defect is now a crack tip moving under the action of a transversal force from left to right by consequently breaking the bonds represented by elastic fuses, see Fig. 6(a).

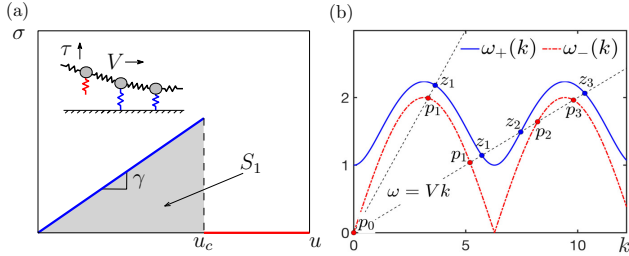


Figure 6: (a) Constitutive relation for a mechanical fuse and schematic representation of a crack propagating with velocity  $V$  under remote load  $\tau$ ; the strain energy jump  $\llbracket w \rrbracket = -S_1$ . (b) Dispersion relations  $\omega_+(k)$  (optical branch) and  $\omega_-(k)$  (acoustic branch) for  $\text{Im}(k) = 0$  characterizing intact and broken lattices, respectively.

The equations governing the evolution of the vertical displacements  $u_j(t)$  are

$$\ddot{u}_j = u_{j-1} + u_{j+1} - 2u_j - \gamma u_j H(u_j - u_c) \quad (11)$$

see Fig. 6(a) for notations, and we again look for solutions in the TW form  $u_j(t) = u(\eta)$ ,  $\eta = j - Vt$ . We need to solve a linear equation  $V^2 u''(\eta) = u(\eta + 1) + u(\eta - 1) - 2u(\eta) - \gamma u(\eta) H(\eta)$  and use the nonlinear switching condition  $u(0) = u_c$  to find the defect velocity  $V$ . The dispersion relations are now represented by one optical branch  $\omega_+^2(k) = 4 \sin^2(k/2) + \gamma$  ahead and one acoustic branch  $\omega_-^2(k) = 4 \sin^2(k/2)$  behind the defect.

One way to solve this more complex problem is to use the Wiener-Hopf technique, see [34] for details. We can again obtain the decomposition  $u(\eta) = u_{in}(\eta) + u_{dr}(\eta)$ , but now to

define different terms we need to introduce two auxiliary functions  $L^{\pm}(k) = L^{\mp 1/2}(k) \exp(\frac{1}{2\pi i} \int_{-\infty}^{\infty} \frac{\text{Log } L(\xi)}{k-\xi} d\xi)$ , where  $L(k) \equiv (\omega_+^2(k) - (kV)^2) / (\omega_-^2(k) - (kV)^2)$ . Then

$$u_{in}(\eta) = \frac{C}{2\pi} \int_{-\infty}^{\infty} \frac{L^{\pm}(k) e^{-ik\eta}}{0 \mp ik} dk, \quad \pm \eta > 0 \quad (12)$$

is the contribution due to remotely applied DC force  $\tau$  which is modeled by the condition that at  $\eta = -\infty$  the time average displacements follows the asymptotics  $u(\eta) \sim -\tau\eta$ , while at  $\eta = +\infty$  the average displacements tend to zero. From these conditions we find that  $C = \tau S \sqrt{(1 - V^2)/\gamma}$  where an explicit expression for the function  $S(V)$  is given in [34]. The contribution due to the AC driving is

$$u_{dr}(\eta) = \frac{1}{2\pi} \int_{-\infty}^{\infty} L^{\pm}(k) \Psi_{dr}^{\pm}(k) e^{-ik\eta} dk, \quad \pm \eta > 0 \quad (13)$$

where

$$\Psi_{dr}^{\pm}(k) = \sum_{j=1}^K \frac{A_j}{2} \left[ \frac{e^{-i(\varphi_j - \pi/2)}}{0 \mp i(k - k_j)} + \frac{e^{i(\varphi_j - \pi/2)}}{0 \mp i(k + k_j)} \right]. \quad (14)$$

Here the wave numbers  $k_j = z_{2j-1}$  describe the sources bringing the energy from  $+\infty$  while the wave numbers  $k_j = p_{2j}$  correspond to sources bringing the energy from  $-\infty$ ; for the cases  $K = 1, 3$  the wave numbers  $z$  and  $p$  are illustrated in Fig. 6(b).

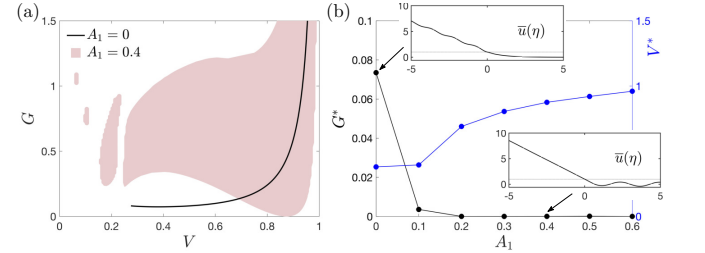


Figure 7: (a) Kinetic domains for admissible solutions with  $K = 1$  and the AC wave coming from ahead. There is only one damping wave in the big pink domain and more than one in the smaller ones. (b) Amplitude dependence of  $G^*(V^*)$  and  $V^*$ . Material properties are  $\gamma = 1$ ,  $u_c = 1$ .

To compute the driving force  $G^M$  we observe that the macroscopic energy dissipation on the crack tip is  $VG^M = \llbracket v^2/2 + \varepsilon^2/2 + w \rrbracket V + \llbracket \bar{\sigma} v \rrbracket$ , where  $w(u) = (1/2)\gamma u^2$  for  $u < u_c$  and  $w(u) = (1/2)\gamma u_c^2$  for  $u > u_c$ . If we now take into consideration the RH compatibility condition  $\llbracket v \rrbracket + V \llbracket \varepsilon \rrbracket = 0$ , we obtain  $VG^M = \llbracket w \rrbracket V + \bar{f} \llbracket v \rrbracket$ . Here  $\bar{f} = \llbracket \bar{\sigma} \rrbracket - V^2 \llbracket \varepsilon \rrbracket$  is the moving concentrated force which represents the microscopic processes in the tip and furnishes the linear momentum RH condition, e.g. [39]. We can now write

$$G^M = \llbracket w \rrbracket - \bar{f} \llbracket \varepsilon \rrbracket \quad (15)$$

and substituting the values  $\varepsilon_- = -\tau$ ,  $\varepsilon_+ = 0$ ,  $\bar{\sigma}(\varepsilon_{\pm}) = \varepsilon_{\pm}$ , we finally obtain  $G^M = \tau^2(1 - V^2)/2 - (\gamma u_c^2)/2$ .

Consider the simplest case when there is only one radiated wave with  $k_1 = p_1$ . The microscopic power exerted by a single AC source ahead of the crack ( $K = 1$ ) is then

$$VG^m = \frac{1}{2}A_1^2\omega_+^2(z_1)|L^+(z_1)|^2|\omega'_+(z_1) - V| \geq 0. \quad (16)$$

The total dissipation  $\mathcal{R}(V) = VG(V) = V(G^M(V) + G^m(V)) \geq 0$  is again a multivalued function of  $V$  as we show in Fig. 7(a); the associated functions  $G^*(V^*)$  and  $V^*$  at different values of  $A_1$  are shown in Fig. 7(b). At a given  $V$  we obtain  $A_1^* = u_c(z_1^2 - p_1^2)/z_1^2$  and  $\varphi_1^* = \pi/2$  with the corresponding dissipation-free solution illustrated in the inset in Fig. 7(b). More general solutions, similar to the ones in Fig. 3, can be obtained as well.

To conclude, we showed that it is possible to fine tune defect kinetics by carefully engineered AC driving. Moreover, using special AC sources on the boundary, one can compensate radiative damping completely, making the crystal free of internal friction for strongly discrete defects. We demonstrated this effect for domain boundaries, dislocations and cracks, however, the obtained results also have important implications for the design of artificial metamaterials supporting mobile topological defects and capable of transporting compact units of mechanical information.

- 
- [1] J. Currie, S. Trullinger, A. Bishop, and J. Krumhansl, *Physical Review B* **15**, 5567 (1977).
- [2] M. Peyrard and M. D. Kruskal, *Physica D: Nonlinear Phenomena* **14**, 88 (1984).
- [3] C. Kunz and J. A. Combs, *Physical Review B* **31**, 527 (1985).
- [4] R. Boesch, C. Willis, and M. El-Batanouny, *Physical Review B* **40**, 2284 (1989).
- [5] P. Kevrekidis, I. Kevrekidis, A. Bishop, and E. Titi, *Physical Review E* **65**, 046613 (2002).
- [6] W. Atkinson and N. Cabrera, *Physical Review* **138**, A763 (1965).
- [7] O. Kresse and L. Truskinovsky, *Journal of the Mechanics and Physics of Solids* **52**, 2521 (2004).
- [8] L. I. Slepyan, in *Doklady Akademii Nauk* (Russian Academy of Sciences, 1981), vol. 258, pp. 561–564.
- [9] M. Marder and S. Gross, *Journal of the Mechanics and Physics of Solids* **43**, 1 (1995).
- [10] L. I. Slepyan, *Journal of the Mechanics and Physics of Solids* **49**, 469 (2001).
- [11] L. Truskinovsky and A. Vainchtein, *SIAM Journal on Applied Mathematics* **66**, 533 (2005).
- [12] T. Dohnal, A. Lamacz, and B. Schweizer, *Asymptotic Analysis* **93**, 21 (2015).
- [13] D. M. Kochmann and K. Bertoldi, *Applied Mechanics Reviews* **69** (2017).
- [14] V. Pfahl, C. Ma, W. Arnold, and K. Samwer, *Journal of Applied Physics* **123**, 035301 (2018).
- [15] R. Capozza, A. Vanossi, A. Vezzani, and S. Zapperi, *Physical Review Letters* **103**, 085502 (2009).
- [16] L. de Arcangelis, E. Lippiello, M. Pica Ciamarra, and A. Sarracino, *Philosophical Transactions of the Royal Society A* **377**, 20170389 (2019).
- [17] S. M. Rubinstein, G. Cohen, and J. Fineberg, *Nature* **430**, 1005 (2004).
- [18] F. Dinelli, S. Biswas, G. Briggs, and O. Kolosov, *Applied Physics Letters* **71**, 1177 (1997).
- [19] C. Winsper, G. Dawson, and D. Sansome, *Metals Materials* **4**, 158 (1970).
- [20] L. L. Bonilla and B. A. Malomed, *Physical Review B* **43**, 11539 (1991).
- [21] D. Cai, A. Bishop, N. Grønbech-Jensen, and B. A. Malomed, *Physical Review E* **50**, R694 (1994).
- [22] B. B. Baizakov, G. Filatrella, and B. A. Malomed, *Physical Review E* **75**, 036604 (2007).
- [23] H. Koizumi, H. Kirchner, and T. Suzuki, *Physical Review B* **65**, 214104 (2002).
- [24] Z. Tshirut, A. Filippov, and M. Urbakh, *Physical Review Letters* **95**, 016101 (2005).
- [25] R. Capozza, S. M. Rubinstein, I. Barel, M. Urbakh, and J. Fineberg, *Physical Review Letters* **107**, 024301 (2011).
- [26] G. S. Mishuris, A. B. Movchan, and L. I. Slepyan, *Journal of the Mechanics and Physics of Solids* **57**, 1958 (2009).
- [27] M. Nieves, G. Mishuris, and L. Slepyan, *International Journal of Solids and Structures* **112**, 185 (2017).
- [28] Y. R. Efendiev and L. Truskinovsky, *Continuum Mechanics and Thermodynamics* **22**, 679 (2010).
- [29] F. Maddalena, D. Percivale, G. Puglisi, and L. Truskinovsky, *Continuum Mechanics and Thermodynamics* **21**, 251 (2009).
- [30] S. Shan, S. H. Kang, J. R. Raney, P. Wang, L. Fang, F. Candido, J. A. Lewis, and K. Bertoldi, *Advanced Materials* **27**, 4296 (2015).
- [31] Y. Zhang, B. Li, Q. Zheng, G. M. Genin, and C. Chen, *Nature Communications* **10**, 1 (2019).
- [32] R. L. Harne and K.-W. Wang, *Harnessing bistable structural dynamics: for vibration control, energy harvesting and sensing* (John Wiley & Sons, 2017).
- [33] L. Slepyan, A. Cherkaev, and E. Cherkaev, *Journal of the Mechanics and Physics of Solids* **53**, 407 (2005).
- [34] See Supplemental Material at [URL will be inserted by publisher] for [give brief description of material].
- [35] C. M. Dafermos, C. M. Dafermos, C. M. Dafermos, G. Mathématicien, C. M. Dafermos, and G. Mathematician, *Hyperbolic conservation laws in continuum physics*, vol. 3 (Springer, 2005).
- [36] L. Truskinovsky, *Journal of Applied Mathematics and Mechanics* **51**, 777 (1987).
- [37] O. Kresse and L. Truskinovsky, *Journal of the Mechanics and Physics of Solids* **51**, 1305 (2003).
- [38] M. Peyrard and A. R. Bishop, *Physical review letters* **62**, 2755 (1989).
- [39] R. Burridge and J. Keller, *SIAM Review* **20**, 31 (1978).

## Supplementary material for the paper: "Frictionless motion of lattice defects"

N.Gorbushin,<sup>1</sup> G. Mishuris,<sup>2</sup> and L. Truskinovsky<sup>1</sup>

<sup>1</sup>PMMH, CNRS – UMR 7636, CNRS, ESPCI Paris, PSL Research University, 10 rue Vauquelin, 75005 Paris, France

<sup>2</sup>Department of Mathematics, Aberystwyth University, Ceredigion SY23 3BZ, Wales, UK

(Dated: June 24, 2020)

### FPU PROBLEM: ANALYTICAL RESULTS

In this problem the characteristic function  $L(k)$  has the following properties:  $L(-k) = L(k)$  and  $L(\bar{k}) = \overline{L(k)}$  and, hence, the real and purely imaginary roots of the characteristic equation  $L(k) = 0$  come in pairs while other complex roots come in quadruplets. Therefore, it is enough to search for the roots of the characteristic equation in the quarter of the complex plane  $\text{Im } k \geq 0$  and  $\text{Re } k \geq 0$ . The associated roots can be conveniently sorted between the sets  $Z^\pm = Z_c^\mp \cup Z_r^\pm$  with  $Z_c^\pm = \{k : L(k) = 0, \pm \text{Im } k > 0\}$  and  $Z_r^\pm = \{|k| > 0 : L(k) = 0, \text{Im } k = 0, \pm kL'(k) > 0\}$ .

With the roots known, the integration in Eq. 2 in the main text can be performed explicitly which allows one to obtain the expression for the full strain field:

$$\varepsilon(\eta) = \begin{cases} \varepsilon_+ + \sum_{j=1}^K A_j \sin(k_j \eta + \varphi_j) - \sum_{k_j \in Z^+} \frac{\sigma_0 \omega^2(k_j)}{k_j L'(k_j)} e^{-ik_j \eta}, & \eta > 0, \\ \varepsilon_- + \sum_{j=1}^K A_j \sin(k_j \eta + \varphi_j) + \sum_{k_j \in Z^-} \frac{\sigma_0 \omega^2(k_j)}{k_j L'(k_j)} e^{-ik_j \eta}, & \eta < 0, \end{cases} \quad (\text{S1})$$

To use the switching condition  $\varepsilon(0) = \varepsilon_c$ , we need to recall the following general properties of the roots of the characteristic equation [1]

$$\sum_{k_j \in Z_c^+} \frac{\omega^2(k_j)}{k_j L'(k_j)} + \sum_{k_j \in Z_c^-} \frac{\omega^2(k_j)}{k_j L'(k_j)} = -\frac{1}{1-V^2} - \sum_{k_j \in Z_r^+} \frac{\omega^2(k_j)}{k_j L'(k_j)} - \sum_{k_j \in Z_r^-} \frac{\omega^2(k_j)}{k_j L'(k_j)}, \quad (\text{S2})$$

$$\sum_{k_j \in Z_c^+} \frac{\omega^2(k_j)}{k_j L'(k_j)} = \sum_{k_j \in Z_c^-} \frac{\omega^2(k_j)}{k_j L'(k_j)}. \quad (\text{S3})$$

We can rewrite the switching condition in two equivalent forms  $\varepsilon_\pm = \varepsilon_c \mp \frac{\sigma_0/2}{1-V^2} + \sigma_0 Q + \sum_{j=1}^K A_j \sin \varphi_j$ , where

$$Q = \frac{1}{2} \sum_{k_j \in Z_r^+} \frac{\omega^2(k_j)}{k_j L'(k_j)} - \frac{1}{2} \sum_{k_j \in Z_r^-} \frac{\omega^2(k_j)}{k_j L'(k_j)}. \quad (\text{S4})$$

Next, we compute the rate of dissipation by lattice waves:

$$\mathcal{R}_\pm = \sum_{k_j \in Z_r^\mp} \langle \mathcal{E}_j \rangle |\omega'(k_j) - V|, \quad (\text{S5})$$

where  $\mathcal{E}_j = v_j^2/2 + w(\varepsilon_j)$  is the energy density carried by the linear wave with the (real) wave number  $k_j > 0$  and  $\omega'(k_j) - V$  is the velocity of the energy drift relative to the velocity of the defect; the signs indicate waves carrying the energy to  $\pm\infty$ . The particle velocity here  $v(\eta) = -V du/d\eta$  can be obtained by inverting the kinematic relation in the Fourier space  $\hat{v}(k) = -V k \exp(ik/2)/[2 \sin(k/2)] \hat{\varepsilon}(k)$ . We obtain explicitly:

$$v(\eta) = \begin{cases} -V\varepsilon_+ - \sum_{j=1}^K \frac{A_j V k_j}{2 \sin(k_j/2)} \sin(k_j(\eta - 1/2) + \varphi_j) + \sum_{k_j \in Z^+} \frac{\sigma_0 V k_j \omega^2(k_j)}{2 k_j \sin(k_j/2) L'(k_j)} e^{-ik_j(\eta-1/2)}, & \eta > 1/2, \\ -V\varepsilon_- - \sum_{j=1}^K \frac{A_j V k_j}{2 \sin(k_j/2)} \sin(k_j(\eta - 1/2) + \varphi_j) - \sum_{k_j \in Z^-} \frac{\sigma_0 V k_j \omega^2(k_j)}{2 k_j \sin(k_j/2) L'(k_j)} e^{-ik_j(\eta-1/2)}, & \eta < 1/2. \end{cases} \quad (\text{S6})$$

After the substitution we obtain

$$G_\pm = \frac{\mathcal{R}_\pm}{V} = \sum_{k_j \in Z_r^\pm, k_j > 0} \left[ \left( \pm 2 \frac{\sigma_0 \omega^2(k_j)}{k_j L'(k_j)} - A_j \sin \varphi_j \right)^2 + A_j^2 \cos^2 \varphi_j \right] \left| \frac{\omega'(k_j)}{V} - 1 \right|. \quad (\text{S7})$$

The first term in the square parenthesis reveals the interaction between the waves generated by AC forces and the waves radiated by the defect. The second term corresponds to the contribution from the AC sources only. If we use the definitions of  $G^M$ , Eq. 4, and  $G^m$ , Eq. 5, in the main text and substitute the expressions of the fields  $\varepsilon(\eta)$  and  $v(\eta)$ , we obtain the relation

$$G^M + G^m = G_+ + G_- . \quad (\text{S8})$$

To verify this identity it is enough to observe that  $2\omega^2(k_j)/(k_j L'(k_j)) = V/(\omega'(k_j) - V)$ . From the representation (S7) it is particularly easy to conclude that the condition  $G^M + G^m = 0$  is satisfied if we set  $\varphi_j = \varphi_j^* = \pi/2$  and amplitudes  $A_j = A_j^* = (-1)^j \sigma_0 V / (\omega'(k_j) - V)$ ,  $j = 1, 2, \dots, K$ .

### FPU PROBLEM: NUMERICAL EXPERIMENTS

To show how the DC and AC driving can be actually implemented and to show stability of the obtained analytical solutions we we conducted a series of direct numerical experiments with a finite chain comprised of  $N = 1001$  masses connected by bi-stable springs.

Our initial conditions contained a pre-existing defect (phase boundary) located at  $n_0 = 200$ . We assigned initial displacements (linear with  $j$ ) in the form  $u_j(0) = \tilde{\varepsilon}_- j$  for  $j \leq n_0$  and  $u_j(0) = \tilde{\varepsilon}_- n_0 + \tilde{\varepsilon}_+ (j - n_0)$  for  $j > n_0$ , where  $\tilde{\varepsilon}_\pm = \varepsilon_c \mp \sigma_0 / 2 + \varepsilon_+ - A/2$ . Here and below, constants  $\varepsilon_\pm$  correspond to the limiting strains and  $A$  is an amplitude of the AC drive which we use in the analytical solution. The initial velocities are set to 0 for each mass:  $\dot{u}_j(0) = 0$ .

We fix the end of the chain on the right side by setting:  $u_{N+1}(t) = u_N(t) + \tilde{\varepsilon}_+$ . The left end is loaded by a constant force  $F = \sigma(\varepsilon_-) + \sigma_0 V / (2(1 + V))$  representing the DC driving so that:  $\ddot{u}_1(t) = \sigma(u_1 - u_2) - FH(t - t_0)$ .

The time shift  $t_0$  is needed for the energy from the AC source to arrive to the defect located at  $n = n_0$ . We associate the AC driving source with the two neighboring masses  $j_0 = 400$  and  $j_0 = 401$  which are located sufficiently far ahead of the initial defect and the right end of a chain. More specifically, we assume that a time periodic pair of force is applied to the spring located between these masses ensuring that the strain in this spring remains the same all the time. The resulting system of equations can be written in the form:

$$\ddot{u}_j(t) = \sigma(u_{j+1} - u_j) - \sigma(u_j - u_{j-1}) - A(\delta_{j j_0} + \delta_{j(j_0+1)}) \sin(\nu t), \quad (\text{S9})$$

where  $\delta_{ij}$  is the Kronecker delta,  $\nu = k_1 V$  and  $k_1$  is the first real positive root of the equation  $L(k) = 0$ .

We performed simulations with 100 transition events taking place before the waves reflected from the boundaries of the chain took any effect. The defect was shown to approach the steady-state TW regime for several values of velocity  $V$  which suggests that the corresponding analytical solution is a dynamic attractor.

Our Fig. 1 shows time evolution of the strain field. The insets in Fig. 1(c) show comparison between the numerically obtained data and the analytical solution for  $A = 0.6$ ,  $V = 0.45$  and  $\varepsilon_- = 2.21$ . In this case  $\varepsilon_+ = -0.29$  and  $G^M + G^m = 0.27$  (the other parameters are  $\sigma_0 = 2$ ,  $\varepsilon_c = 1$ ). In the attached Movie 1 we show the dynamic propagation of the phase boundary as

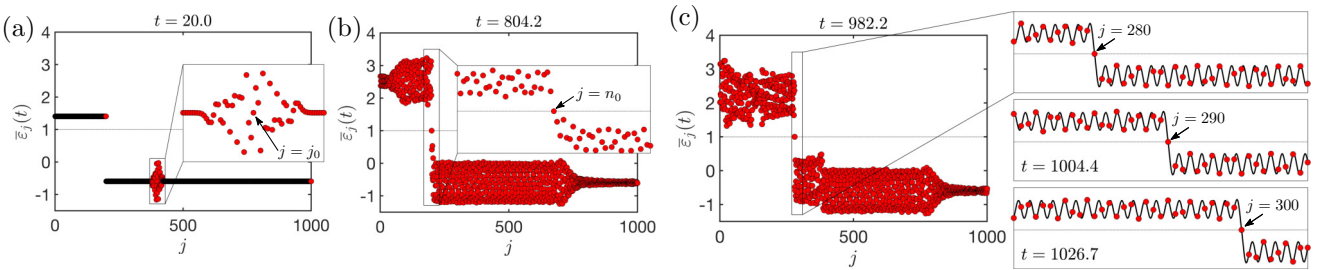


Figure 1: Snapshots of the normalized strains  $\bar{\varepsilon}_j(t) = \varepsilon_j(t)/\varepsilon_c$  at different moments: (a) initial propagation of the wave from the AC forces centred at  $j = j_0 = 400$  and  $j_0 + 1$ ; the initial defect is at  $j = n_0 = 200$ ; (b) the first transition event takes place at  $j = n_0$  soon after the energy from the DC force (turned on at  $t = t_0 = 600$ ) at the left end arrived; (c) steady-state propagation achieved when the comparison with the analytical solution (black solid lines) is possible; the insets on the right show snapshots of strains when the front is at  $j = 280, 290$  and  $300$ .

demonstrated in the insets of Fig. 1(c). The numerical solution is interposed with the analytical solution of the front moving at  $V = 0.45$ . During the propagation of the defect, the points progressively move from the phase with  $\varepsilon_+$  to the phase with  $\varepsilon_-$  by passing  $\varepsilon_c$ . The trajectories follow precisely the analytical solution.

To show stability of the frictionless solutions we performed numerical simulations with initial conditions corresponding to the analytical solution (S1). The time dependent problem  $\ddot{\varepsilon}_j = \sigma(\varepsilon_{j+1}) + \sigma(\varepsilon_{j-1}) - 2\sigma(\varepsilon_j)$  was solved while the ends of the

chain were let free:  $\ddot{\varepsilon}_1 = \sigma(\varepsilon_2) - 2\sigma(\varepsilon_1)$  and  $\ddot{\varepsilon}_N = \sigma(\varepsilon_{N-1}) - 2\sigma(\varepsilon_N)$  with  $N = 1000$ . The initial position of the defect was set in the middle of the chain at  $n_0 = 500$ . The snapshots of the moving front for this case are shown in Fig. 2 where the propagation speed is  $V = 0.5$ . The attached Movie 2 demonstrates transient propagation of the defect shown in Fig. 2. We see that the analytically predicted velocity  $V$  is maintained and the time dependence of strains follow the analytical solution.

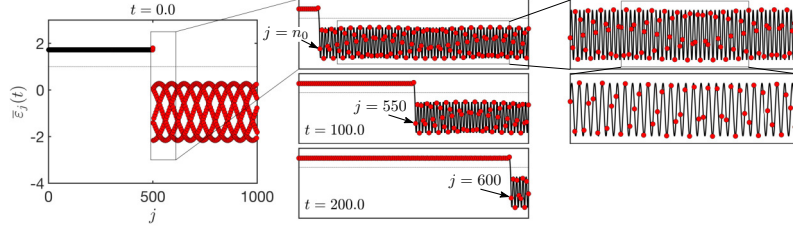


Figure 2: Normalized strains  $\bar{\varepsilon}_j(t) = \varepsilon_j(t)/\varepsilon_c$  at different moments with the initial data corresponding to the TW solution (S1) with the initial front position at  $j = n_0 = 500$  and propagation speed  $V = 0.5$ . The inserts show comparison with the analytical results (black solid lines).

### FK PROBLEM: ANALYTICAL RESULTS

By performing integration in Eq. 7 in the main text we obtain the expression for the displacement field

$$u(\eta) = \begin{cases} u_+ + \sum_{j=1}^K A_j \sin(k_j \eta + \varphi_j) - \sum_{k_j \in Z^+} \frac{\sigma_0}{k_j L'(k_j)} e^{-ik_j \eta}, & \eta > 0, \\ u_- + \sum_{j=1}^K A_j \sin(k_j \eta + \varphi_j) + \sum_{k_j \in Z^-} \frac{\sigma_0}{k_j L'(k_j)} e^{-ik_j \eta}, & \eta < 0. \end{cases} \quad (\text{S10})$$

The sets  $Z^\pm$  are defined in the same way as in the FPU problem.

The switching condition  $u(0) = u_c$  can be again written in two equivalent forms  $u_\pm = u_c \mp (\sigma_0/2) + \sigma_0 R - \sum_j A_j \sin \varphi_j$ , where

$$R = \frac{1}{2} \sum_{k_j \in Z_r^+} \frac{1}{k_j L'(k_j)} - \frac{1}{2} \sum_{k_j \in Z_r^-} \frac{1}{k_j L'(k_j)}. \quad (\text{S11})$$

Next we compute the rate of energy dissipation  $\mathcal{R}_\pm = G_\pm V$  following the same methodology as in the FPU problem. We obtain:

$$G_\pm = \sum_{k_j \in Z_r^\pm, k_j > 0} \left[ \left( \pm 2 \frac{\sigma_0}{k_j L'(k_j)} - A_j \sin \varphi_j \right)^2 + A_j^2 \cos^2 \varphi_j \right] \omega^2(k_j) \left| \frac{\omega'(k_j)}{V} - 1 \right|. \quad (\text{S12})$$

The energy balance (S8) remains the same and can be again verified by direct substitution. From (S12) one can see that the choice  $\varphi_j = \varphi_j^* = \pi/2$  and  $A_j = A_j^* = (-1)^j \sigma_0 V / (\omega(k_j)^2 (\omega'(k_j) - V))$ ,  $j = 1, 2, \dots, K$  ensures frictionless propagation of the defect.

### PB PROBLEM: ANALYTICAL RESULTS

With the TW ansatz applied, the Fourier transform reduces Eq. 11 to

$$L(k) \hat{u}^+(k) + \hat{u}^-(k) = \frac{\hat{q}(k)}{\omega_-^2(k) - (Vk)^2}, \quad (\text{S13})$$

where superscripts  $\pm$  define complex-valued functions which are analytic in the half-planes  $\pm \text{Im } k > 0$ , respectively. To represent the external DC/AC driving on the boundary of the chain, the function  $\hat{q}(k)$  must be chosen to have a zero physical space image  $q(\eta) \equiv 0$ . The kernel function  $L(k) = (\omega_+^2(k) - (Vk)^2) / (\omega_-^2(k) - (Vk)^2)$  has zeros  $z_j$  (roots of  $\omega_+^2(z_j) = (Vz_j)^2$ ) and poles  $p_j$  (roots of  $\omega_-^2(p_j) = (Vp_j)^2$ ). The symmetry properties  $L(-k) = L(k)$  and  $L(\bar{k}) = \overline{L(k)}$



remain here the same as in FPU and FK problems. We can then define the sets of poles  $P^\pm = P_c^\mp \cup P_r^\pm$  such that  $P_c^\pm = \{p : \omega_+^2(p) - (pV)^2 = 0, \pm \text{Im } p > 0\}$  and  $P_r^\pm = \{p > 0 : \omega_+^2(p) - (pV)^2 = 0, \text{Im } p = 0, \pm(\omega'_-(p) - V) > 0\}$ . Similarly, we define the sets of zeros:  $Z^\pm = Z_c^\mp \cup Z_r^\pm$  with  $Z_c^\pm = \{z : \omega_+^2(z) - (zV)^2 = 0, \pm \text{Im } z > 0\}$  and  $Z_r^\pm = \{z > 0 : \omega_+^2(z) - (zV)^2 = 0, \text{Im } z = 0, \pm(\omega'_+(z) - V) > 0\}$ .

The problem (S13) can be solved using the Wiener-Hopf technique [2]. The main step is the factorization of the function  $L(k) = L^-(k)/L^+(k)$ . The standard factorization formula gives on the real line

$$L^\pm(k) = L^{\mp 1/2}(k) \exp\left(-\frac{1}{2\pi i} \text{p.v.} \int_{-\infty}^{\infty} \frac{\text{Log } L(\xi)}{\xi - k} d\xi\right) \quad (\text{S14})$$

We can alternatively apply the Weierstrass factorization theorem and present the factors as infinite products [2]. Then we obtain the representation

$$L^\pm(k) = \left(\frac{\gamma}{1-V^2}\right)^{\mp 1/2} (0 \mp ik)^{\pm 1} \left[ \frac{\prod_{z_j \in Z_r^\pm} (1 - (k/z_j)^2) \prod_{z_j \in Z_c^\pm} (1 - (k/z_j))}{\prod_{p_j \in P_r^\pm} (1 - (k/p_j)^2) \prod_{p_j \in P_c^\pm} (1 - (k/p_j))} \right]^{\mp 1} \frac{1}{S}, \quad (\text{S15})$$

where for future convenience we defined

$$S = \frac{\prod_{z_j \in Z_r^+} z_j \prod_{z_j \in Z_r^-} z_j}{\prod_{p_j \in P_r^-} p_j \prod_{p_j \in P_r^+} p_j}. \quad (\text{S16})$$

These expressions can be evaluated if we know the location of the zeros  $z_j$  and the poles  $p_j$  introduced above.

We can now rewrite the left hand side of (S13) as a sum of "+" and "-" functions that are analytic in the upper and lower half plane, respectively:

$$\frac{1}{L^+(k)} \hat{u}^+(k) + \frac{1}{L^-(k)} \hat{u}^-(k) = \Psi(k). \quad (\text{S17})$$

The explicit solution of (S17) can be now obtained by decomposing the right hand side

$$\Psi(k) = \frac{1}{L^-(k)} \frac{\hat{q}(k)}{\omega_-^2(k) - (Vk)^2} \quad (\text{S18})$$

into a sum of "+" and "-" functions. To represent the general DC and AC sources we can set

$$\Psi(k) = 2\pi C \delta(k) + 2\pi \sum_{k_j} C_j \delta(k - k_j), \quad (\text{S19})$$

where the wave numbers  $k_j$  are chosen from the set  $Z_r^-$  if the AC source is located ahead of the defect and from the set  $P_r^+$  if the source is behind the defect. Since  $L^-(k_j) [\omega_-^2(k_j) - (Vk_j)^2] = 0$ , we have  $q(\eta) = 0$  and the sources, parametrized by the constants  $C$  (DC driving) and  $C_j$  (AC driving), are indeed invisible in the bulk.

If we further additively factorize the delta functions  $\delta(k - k_j) = 2\pi [1/(0 + i(k - k_j)) + 1/(0 - i(k + k_j))]$  we can write

$$\Psi(k) = \Psi^+(k) + \Psi^-(k), \quad \Psi^\pm(k) = \frac{C}{0 \mp ik} + \sum_{k_j \in Z_r^- \cup P_r^+} \frac{A_j}{2} \left[ \frac{e^{-i(\varphi_j - \pi/2)}}{0 \mp i(k - k_j)} + \frac{e^{i(\varphi_j - \pi/2)}}{0 \mp i(k + k_j)} \right]. \quad (\text{S20})$$

In this representation the complex amplitudes  $C_j$  are replaced by the real amplitudes  $A_j$  and real phases  $\varphi_j$ . The total number of the corresponding sinusoidal waves is  $K = |Z_r^-| + |P_r^+|$ .

We can now apply the Liouville theorem [2] to (S17) and obtain the explicit solution of our problem  $\hat{u}^\pm(k) = L^\pm(k) \Psi^\pm(k)$ . Given that  $\hat{u}(k) = \hat{u}^+(k) + \hat{u}^-(k)$  we obtain in the physical space  $u(\eta) = \frac{1}{2\pi} \int_{-\infty}^{\infty} L^\pm(k) \Psi^\pm(k) e^{-ik\eta} dk$ , when  $\pm\eta > 0$ , respectively, which gives Eq. 12 and Eq. 13 in the main text. We can now apply the switching condition to obtain  $C + \sum_{j=1}^K A_j \sin \varphi_j = u_c$ . Then using the boundary condition at  $-\infty$  we obtain the link between the constant  $C$  and the amplitude of the DC driving  $\tau$  in the form  $\tau = (C/S(V)) \sqrt{(1-V^2)/\gamma}$ . In the physical space the ensuing solution takes a form  $u^\pm(\eta) = u_1^\pm(\eta) + u_2^\pm(\eta)$ , for  $\eta$  larger (smaller) than 0, respectively. Here

$$u_1^\pm(\eta) = \sum_{z_j \in Z_r^+ / P_r^-} \alpha_j^\pm \cos(z_j \eta + \beta_j^\pm) + \sum_{z_j \in Z_c^+ / P_c^-} \alpha_j^\pm e^{-i(z_j \eta + \beta_j^\pm)} \quad (\text{S21})$$

are the terms which do not contain DC/AC driving amplitudes explicitly. However, in contrast to the previous cases, the implicit dependence is present through the real coefficients  $\alpha_j^\pm$  and  $\beta_j^\pm$  representing the complex numbers:

$$\alpha_j^\pm e^{-i\beta_j^\pm} = \frac{i\Psi^\pm(k_j)L^\mp(k_j)\gamma}{2k_jV(\omega'_\pm(k_j) - V)}, \quad (\text{S22})$$

where  $k_j = z_j$  when the sign is + and  $k_j = p_j$  if it is -. The part of the solution explicitly related to external driving can be in turn split into a DC and an AC related parts:  $u_2^\pm(\eta) = u_{DC}^\pm(\eta) + u_{AC}^\pm(\eta)$ . Here  $u_{DC}^+(\eta) = 0$  and

$$u_{DC}^-(\eta) = \frac{C}{S} \sqrt{\frac{1-V^2}{\gamma}} \left[ \left( \sum_{z_j \in Z_c^-} \frac{i}{z_j} - \sum_{p_j \in P_c^-} \frac{i}{p_j} \right) - \eta \right]. \quad (\text{S23})$$

The AC related term is

$$u_{AC}^\pm(\eta) = \sum_{k_j \in Z_r^- / P_r^+} A_j |L^\pm(k_j)| \sin(k_j\eta + \varphi_j - \arg L^\pm(k_j)). \quad (\text{S24})$$

In the main text we showed that in this problem the macro-level energy release rate is  $VG^M(V) = (\tau^2(1-V^2)/2 - (\gamma u_c^2)/2)V$  while the rate of dissipation due to the AC driving is:

$$VG^m(V) = \sum_{z_j \in Z_r^-} \frac{A_j^2 |L^+(z_j)|^2}{2} \omega_+^2(z_j) (V - \omega'_+(z_j)) + \sum_{p_j \in P_r^+} \frac{A_j^2 |L^-(p_j)|^2}{2} \omega_-^2(p_j) (\omega'_-(p_j) - V). \quad (\text{S25})$$

The dissipation due to radiated elastic waves is:

$$VG_+(V) = \sum_{z_j \in Z_r^+} \frac{(\alpha_j^+)^2}{2} \omega_+^2(z_j) (\omega'_+(z_j) - V), \quad VG_-(V) = \sum_{p_j \in P_r^-} \frac{(\alpha_j^-)^2}{2} \omega_-^2(p_j) (V - \omega'_-(p_j)). \quad (\text{S26})$$

The validity of the energy balance (S8) in this case was checked numerically for the whole range of velocity  $0 < V < 1$ .

The total dissipation becomes equal to zero if  $\alpha_j^+ = 0$  and  $\alpha_j^- = 0$  which can be ensured if we adjust the amplitudes  $A_j$  in such a way that  $\Psi^+(z_j) = 0$  and  $\Psi^-(p_j) = 0$ . These conditions can be rewritten as a linear system for the amplitudes  $A_j$ :

$$\sum_{k_j \in Z_r^- \cup P_r^+} A_j \frac{k_j^2}{k_j^2 - p_i^2} = u_c, \quad p_i \in P_r^-, \quad \sum_{k_j \in Z_r^- \cup P_r^+} A_j \frac{k_j^2}{k_j^2 - z_i^2} = u_c, \quad z_i \in Z_r^+ \quad (\text{S27})$$

with additional requirement that  $\varphi_j = \varphi_j^* = \pi/2$ .

---

[1] L. Truskinovsky and A. Vainchtein, *SIAM Journal on Applied Mathematics* **66**, 533 (2005).

[2] B. Noble, *Methods based on the Wiener-Hopf technique for the solution of partial differential equations* (1958).